



Changes in grey matter volume and functional connectivity in cluster headache versus migraine

Antonio Giorgio¹ · Chiara Lupi² · Jian Zhang¹ · Francesco De Cesaris² · Mario Alessandri² · Marzia Mortilla³ · Antonio Federico¹ · Pierangelo Geppetti² · Nicola De Stefano¹ · Silvia Benemei²

© Springer Science+Business Media, LLC, part of Springer Nature 2019

Abstract

Cluster headache (CH) shows a more severe clinical picture than migraine (Mig). We tested whether brain changes can explain such difference. Multimodal MRI was acquired in attack-free patients with CH ($n = 12$), Mig ($n = 13$) and in normal controls (NC, $n = 13$). We used FSL for MRI data analysis and nonparametric permutation testing for voxelwise analyses ($p < 0.01$, corrected). CH showed lower grey matter (GM) volume, compared to Mig and NC, in frontal cortex regions (inferior frontal gyrus and frontal pole [FP], respectively) and, only compared to Mig, in lateral occipital cortex (LOC). Functional connectivity (FC) of CH was higher than Mig and NC within working memory and executive control networks and, only compared to Mig, between cerebellar and auditory language comprehension networks. In the attack-free state, the CH brain seems to be characterized by: (i) GM volume decrease, compared to both Mig and NC, in pain modulation regions (FP) and, only with respect to Mig, in a region of visual processing modulation during pain and working memory (LOC); (ii) increased FC at short range compared to both Mig and NC and at long range only with respect to Mig, in key cognitive networks, likely due to maladaptation towards more severe pain experience.

Keywords Cluster headache · Migraine · MRI · Volumetry · Connectivity

Co-investigators Alberto Chiarugi (Headache Centre, Careggi University Hospital, Department of Health Sciences, University of Florence, Florence, Italy)

Antonio Giorgio and Chiara Lupi contributed equally to this work

✉ Antonio Giorgio
giorgio3@unisi.it

Chiara Lupi
chiara.lupi@unifi.it

Jian Zhang
zhangjianeave@gmail.com

Francesco De Cesaris
f.decesaris@unifi.it

Mario Alessandri
mralessandri@gmail.com

Marzia Mortilla
marzia.mortilla@meyer.it

Antonio Federico
federico@unisi.it

Pierangelo Geppetti
geppetti@unifi.it

Nicola De Stefano
destefano@unisi.it

Silvia Benemei
silvia.benemei@unifi.it

¹ Department of Medicine, Surgery and Neuroscience, University of Siena, Viale Bracci 2, 53100 Siena, Italy

² Headache Centre, Careggi University Hospital, Department of Health Sciences, University of Florence, Florence, Italy

³ Anna Meyer Children's University Hospital, Florence, Italy

Introduction

Cluster headache (CH) and migraine (Mig) are distinct and potentially disabling primary headaches, accompanied by sensory, cognitive and emotional dysfunction ((IHS) 2013), supporting a diffuse involvement of the brain. A more severe clinical picture than Mig characterizes CH, with excruciatingly painful, mostly unilateral headache attacks typically accompanied by trigeminal autonomic symptoms. MRI studies on patients during interictal period revealed contradictory findings in both headache conditions. Mig patients showed, compared to normal controls (NC), decreased (Kim et al. 2008; Rocca et al. 2006; Valfre et al. 2008) and/or increased (Granziera et al. 2006; Messina et al. 2013; Rocca et al. 2006) measures of regional grey matter (GM) volumetry (i.e., volume, thickness, surface area), presence (Hadjipavlou et al. 2006; Yu et al. 2013; Yuan et al. 2012) or absence (Neeb et al. 2015) of abnormal diffusion tensor imaging (DTI)-derived anatomical connectivity along white matter (WM) tracts and both decreased and increased resting functional MRI (fMRI)-derived regional functional connectivity (Chen et al. 2016; Jin et al. 2013; Yu et al. 2017; Yuan et al. 2012).

Inconsistent findings were also reported in CH patients, with respect to NC, in terms of bidirectional changes of GM volume and anatomical connectivity along WM tracts (Absinta et al. 2012; Chou et al. 2014; Szabo et al. 2013; Teepker et al. 2012). Moreover, few resting fMRI studies in interictal CH demonstrated, through a simple region-of-interest approach, abnormal functional connectivity of the hypothalamus extending beyond the traditional pain matrix (Qiu et al. 2013; Yang et al. 2014).

To date, except a study assessing hypothalamic GM volume (Arkink et al. 2017), no direct comparison has been performed between CH and Mig patients to assess differences in both structural and functional brain changes. Thus, no scientific evidence exists of a possible disease-specific “signature” translating a clinical into a brain phenotype. Multimodal and advanced MRI techniques investigating both structural and functional features across the brain could help elucidate whether a different pathophysiology between these two headache types really exists, with the potential to help identify new therapeutic targets.

Using this background, we sought to investigate, at both structural and functional levels, the brain changes explaining the more severe clinical picture in CH compared to Mig.

Methods

Study subjects

We performed a cross-sectional case-control study, with three age-matched cohorts of CH, Mig and NC.

Patients (>18 years old), diagnosed with episodic CH or Mig without aura, according to the International Classification of Headache Disorders criteria ((IHS) 2013), were informed about the study during regular visits at the Headache Centre of the Careggi University Hospital, Florence. At study entry, none of the patients were on preventive treatment, because of 1 month or more without cluster for CH patients, or low frequency of migraine attacks, whose resolution had occurred at least 3 days before, for Mig patients. Before MRI, a headache physician assessed all patients clinically. NC group was made up of healthy subjects recruited among laboratory and hospital workers, and without history of headache, neurological or psychiatric disorders.

Exclusion criteria for all participants were age > 60 years, contraindications to MR examination, arterial hypertension, diabetes and history of cerebrovascular or cardiovascular disease, cognitive impairment (scoring on the Mini Mental State Examination [MMSE] <25).

Forty-seven subjects were enrolled (CH, $n = 15$; Mig, $n = 18$; NC, $n = 14$). However, eight subjects were excluded from the study because of enrollment errors (age out of range [$n = 3$], presence of aura [$n = 1$]), gross movement artifacts ($n = 2$), incidental MRI findings ($n = 2$), and one patient did not complete the MRI examination because of ensuing claustrophobia.

Finally, MRI analysis was performed on 12 CH patients (40 ± 8.1 years old; 8 males), and 13 Mig patients (38.4 ± 6.8 years old; 5 males), both free from attacks and preventive treatment, and 13 NC (41.6 ± 10 years old; 8 males). Clinical and demographic characteristics of headache patients are reported in Table 1.

MRI acquisition

Brain MRI was acquired on a 3 T Philips scanner (Philips Medical Systems, Best, The Netherlands) located at Meyer University Hospital, Florence, during the scan time of the Quantitative Neuroimaging Laboratory (QNL) of the University of Siena. A sagittal survey image was used to identify the anterior and posterior commissures. Sequences were acquired in the axial plane parallel to the bicommissural line. A FLAIR image (repetition time [TR] = 11,000 ms, echo time [TE] = 125 ms, inversion time = 2800 ms, voxel size = $1 \times 1 \times 3$ mm) was acquired for WM hyperintensities (WMH) assessment. DTI data consisted of echo-planar imaging (EPI) (TR =

Table 1 Clinico-demographic and WMH characteristics of cluster headache (CH) and migraine without aura (Mig) patients

	CH (<i>n</i> = 12)	Mig (<i>n</i> = 13)
Age (years)	40 ± 8.1	38.4 ± 6.8
Sex	8 males	5 males
Cluster bouts/year	0.93 ± 0.56	n.a.
Cluster bout duration (days)	56.3 ± 40.7	n.a.
CH attacks/day	2.17 ± 0.81	n.a.
Migraine attacks/month	n.a.	2.48 ± 2.64
Headache attack duration (hours)	1.37 ± 0.77	19.17 ± 18.08
Pain intensity (NRS*)	10 (<i>n</i> = 12)	4 (<i>n</i> = 3) 5 (2) 7 (6) 8 (2)
Pain side	left (<i>n</i> = 2), right (<i>n</i> = 10)	left (<i>n</i> = 1) right (<i>n</i> = 1) left or right (<i>n</i> = 4) bilateral (<i>n</i> = 7)
WMH		
Number	0.75 ± 0.76	1.53 ± 1.89
Volume (cm ³)	0.06 ± 0.15	0.10 ± 0.18

Continuous data are reported as mean ± standard deviation

n.a. not applicable, *NRS* Numeric Rating Scale, *WMH* white matter hyperintensities

7036 ms; TE = 196 ms; voxel size = 2.5 mm³), with 32 diffusion directions and b-value = 900 s/mm². The resting-fMRI data were 200 volumes of EPI sequence with TR = 3000 ms, TE = 35 ms, voxel size = 1.87 × 1.87 × 4 mm. A high-resolution T1-weighted image (TR = 10 ms, TE = 4 ms, voxel size = 1 mm³) was also acquired for image registration, anatomical mapping, and analysis of GM volume.

MRI analysis

MRI analysis was performed at the Quantitative Neuroimaging Lab (QNL) of the University of Siena, mainly using tools of FSL (FMRIB Software Library, Oxford, UK, www.fmrib.ox.ac.uk/fsl/).

Macroscopic brain findings

A single observer with longstanding MRI experience (A.G.) visually assessed FLAIR images for the possible presence of WMH, which were scored on the Fazekas scale (Fazekas et al. 1987) and outlined using a semiautomated segmentation technique based on user-supervised local thresholding (Jim; www.xinapse.com/Manual/).

Voxelwise analysis of GM volumes

Voxelwise analysis of GM volumes was performed on 3D T1-weighted images with FSL-voxel based morphometry (VBM), which uses an optimized VBM protocol. Briefly, T1-W images were brain-extracted, GM-segmented, and registered onto the MNI152 standard space using FNIRT nonlinear registration. Then, all native GM images were nonlinearly registered onto a symmetric study-specific GM template, modulated and smoothed (isotropic Gaussian kernel, sigma = 3 mm). Finally, voxelwise group statistics was performed (see [Statistics](#) paragraph).

Voxelwise analysis of DTI data

DTI data were preprocessed through automatic quality control performed with DTIPrep (www.nitrc.org/projects/dtiprep/), a tool that minimizes various types of artifacts (Oguz et al. 2014). Then, analysis was performed across the whole brain with FSL. Briefly, we used FDT (FMRIB Diffusion Toolbox) to obtain, by fitting a diffusion tensor model to the raw DTI data, images of fractional anisotropy (FA), axial diffusivity (AD), radial diffusivity (RD) and mean diffusivity (MD). The subsequent analysis was performed with TBSS (Tract-Based Spatial Statistics). Briefly, DTI images were registered onto a common standard space (FMRI58_FA) using FNIRT nonlinear registration and, from the mean FA images, the mean WM “skeleton” (thresholded at FA > 0.2) was created, representing the centers of all tracts common to the whole study population, onto which registered DTI images were projected. Finally, voxelwise group statistics was performed (see [Statistics](#) paragraph).

Voxelwise analysis of resting fMRI

Various preprocessing steps were performed for each resting fMRI image: removal of the first 5 volumes to allow signal stability; initial motion correction by volume-realignment to the middle volume using linear registration MCFLIRT (Jenkinson and Smith 2001); non-brain removal using BET; global 4D mean intensity normalization; spatial smoothing (6 mm FWHM); registration to the T1-weighted image using the affine “boundary-based registration” cost of FLIRT (Jenkinson and Smith 2001), and subsequent transformation to MNI152 standard space using FNIRT nonlinear registration (warp resolution: 10 mm); use of ICA-AROMA (independent component analysis-based automatic removal of motion artifacts) in order to minimize motion-related artifacts (Pruim et al. 2015); regression of WM and cerebrospinal fluid (CSF) (both thresholded at a very conservative threshold of 95% tissue probability) in order to remove

residual structured noise; application of a high-pass temporal filtering (cut-off frequency = 100 s); final normalization to MNI152 standard space using FNIRT. The filtered, normalized fMRI images of all study subjects were concatenated across time into a single 4D image, which was then automatically decomposed by MELODIC (multivariate exploratory linear optimized decomposition into independent components [ICs]) into a set of 45 ICs. Finally, voxelwise intranetwork (short-range) functional connectivity analysis was performed using the “dual-regression” approach. The outputs of the first-stage dual regression (i.e., the subject-specific timeseries) were used for estimating temporal correlation between all the RSNs pairs, which is a measure of internetwork (or long-range) functional connectivity strength, using FSLNets. All internetwork Pearson correlation coefficients were transformed into z-scores using the Fisher transform to improve data normality, and then clustered hierarchically for each of the three group comparisons, thus leading to different functional groupings of the RSNs. Full correlation allows for the influence of other networks on RSN pairs while partial correlation represents a more direct relationship between RSN pairs.

Statistics

Differences among the three study groups were assessed, using SPSS (v20, IBM), with analysis of variance (ANOVA) for age, with Chi-square for sex and WMH presence whereas the Mann-Whitney test was used for the comparison of WMH number and volume and of disease duration between the two patient groups.

Voxelwise group differences across the whole brain were performed in the general linear model (GLM) framework with ANOVA (F-test followed by post-hoc pair comparisons of CH, Mig and NC) using “randomise”, a nonparametric

permutation testing ($n = 5000$). Thresholding of statistical images was performed with “threshold-free cluster enhancement” (TFCE), with a significance level of $p \leq 0.01$, corrected for multiple comparisons across space. Age and sex were set as covariates in all analyses. WM and GM regions corresponding to local maxima within significant clusters were anatomically mapped using FSL standard-space atlases (Harvard-Oxford cortical/subcortical structural atlases for GM, JHU DTI-based WM atlases for WM).

Results

There was no group heterogeneity in terms of age ($p = 0.64$), sex ($p = 0.31$), presence, number and volume of WMH ($p > 0.20$ for all) which, when present, were few in number and small in volume (grade 1 on the Fazekas scale). Global cognition was normal in all study subjects (MMSE, corrected for age and education: 28.6 ± 1.2 in CH, 29.7 ± 0.63 in Mig, 29.4 ± 1.2 in NC).

Regional grey matter volume

Group heterogeneity was found (ANOVA, $p \leq 0.01$). Compared to NC, GM density was lower in the inferior frontal gyrus of CH (0.33 ± 0.07 vs 0.43 ± 0.06 , $p = 0.001$) and in the lingual gyrus of Mig (0.40 ± 0.07 vs 0.54 ± 0.08 , $p < 0.001$). Moreover, higher GM density than NC occurred in CH in the cerebellum and occipital fusiform gyrus (0.61 ± 0.08 vs 0.53 ± 0.08 , $p = 0.01$) and in Mig in the lateral occipital cortex (0.41 ± 0.05 vs 0.31 ± 0.03 , $p < 0.001$).

Compared to Mig, GM density of CH was lower in the frontal pole and superior lateral occipital cortex (0.39 ± 0.04 vs 0.50 ± 0.06 , $p < 0.001$) (Fig. 1; Table 2A).

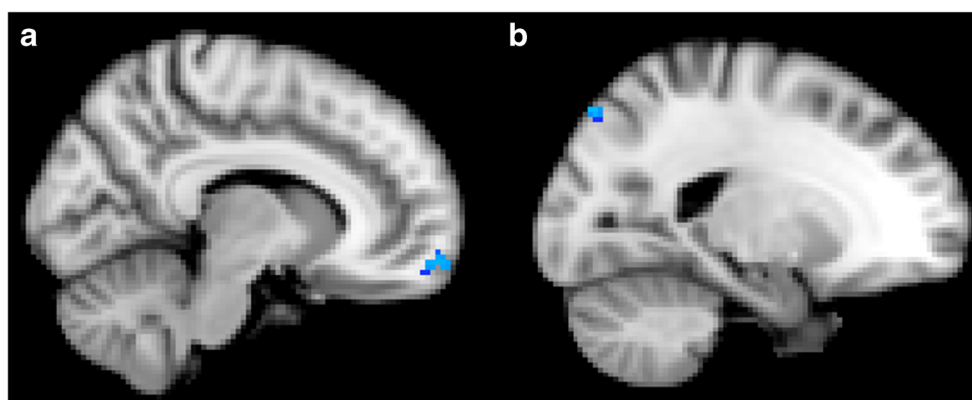


Fig. 1 FSL-Voxel Based Morphometry comparison between cluster headache and migraine groups. Light-blue shows the clusters where the former group has lower (ANOVA, $p \leq 0.01$ corrected) grey matter volume than the latter group, mapping on the frontal pole (a) and superior division

of the lateral occipital cortex (b). Background image is the MNI standard brain in radiological convention. The most informative slices are shown. See text for details

Table 2 Cortical GM regions where CH patients showed lower volume (A) and higher functional connectivity than Mig patients (ANOVA, $p \leq 0.01$, corrected)

GM regions (local maxima)	Side	MNI X,Y,Z (mm)	Cluster size (voxel number)	<i>P</i> value
A (volume)				
Frontal pole	R	8,60,-12	58	0.01
Lateral occipital cortex (superior division)	L	-22,-80, 50	24	0.01
B (functional connectivity)				
Middle frontal gyrus (working memory network)	R	34,-2,64	10	0.01
Frontal pole (executive control network)	R	38,38,38	10	0.01

Anatomical connectivity along white matter tracts

In terms of group heterogeneity (ANOVA), none of the DTI measures (FA, AD, RD and MD) survived statistical correction.

Functional connectivity at the level of brain networks

Across the whole study population, 27 functionally relevant resting state networks (RSNs, main networks and subnetworks) were found, including the default mode network ($n = 3$), executive control network ($n = 2$), frontoparietal working memory network ($n = 2$), ventral and dorsal attention network ($n = 4$), sensorimotor network ($n = 4$), primary and secondary visual network ($n = 7$), auditory language comprehension network ($n = 1$), basal ganglia network ($n = 1$), cerebellar network ($n = 2$), and middle temporal lobe network ($n = 1$).

Group heterogeneity (ANOVA, $p \leq 0.01$) was found for both types of functional connectivity.

In terms of short-range functional connectivity, this was higher in CH than in NC in various brain networks, including the working memory network (inferior frontal gyrus, 17.2 ± 13.5 vs -2.3 ± 2.4 , $p = 0.001$), executive control network (superior frontal gyrus, 8.05 ± 7.37 vs -2.6 ± 5.07 , $p < 0.001$) and default mode network (superior parietal lobule, 9.67 ± 6.2 vs -2.6 ± 5.2 , $p < 0.001$). Mig showed, with respect to NC,

altered functional connectivity in the default mode network, with lateral increase (angular gyrus, 11.2 ± 7.8 vs -2.49 ± 5.1 , $p < 0.001$) and medial decrease (precuneus cortex, -8.7 ± 6.76 vs 6.4 ± 9.5 , $p < 0.001$), and lower functional connectivity in the working memory network (middle frontal gyrus, -0.5 ± 3.4 vs 7.6 ± 7.6 , $p = 0.001$). Similarly to the comparison with NC, functional connectivity of CH was higher than Mig in the working memory network (middle frontal gyrus, 20.16 ± 13.94 vs 2.15 ± 8 , $p = 0.001$) (Fig. 2a; Table 2) and executive control network (frontal pole, 21.5 ± 13.12 vs 5.18 ± 5.27 , $p = 0.001$) (Fig. 2b; Table 2).

As for long-range functional connectivity, CH showed higher partial correlation (i.e., direct relationship) between the cerebellar network and auditory language comprehension network compared to Mig (median [range]: 0.64 [-0.54 to 1.57] vs -0.56 [-1.53 to 0.47], $p = 0.0044$) (Fig. 3). No significant results were found in the comparisons of NC with the two patient groups.

Discussion

In this study we assessed MRI-derived measures of structural brain damage and functional connectivity changes in CH patients, out of bouts and not on preventive treatment compared

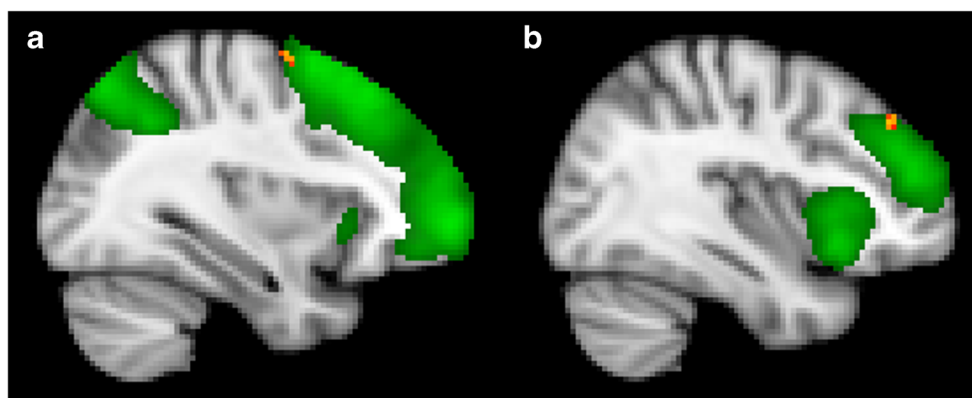


Fig. 2 Differences in within-network (short-range) functional connectivity between cluster headache and migraine groups. Red-yellow shows clusters where the former group has higher (ANOVA, $p \leq 0.01$ corrected) functional connectivity than the latter in brain

networks (in green), including working memory network (a) and executive control network (b). Background image, shown in radiological convention, is the standard MNI brain. The most informative slices are shown. See text for details

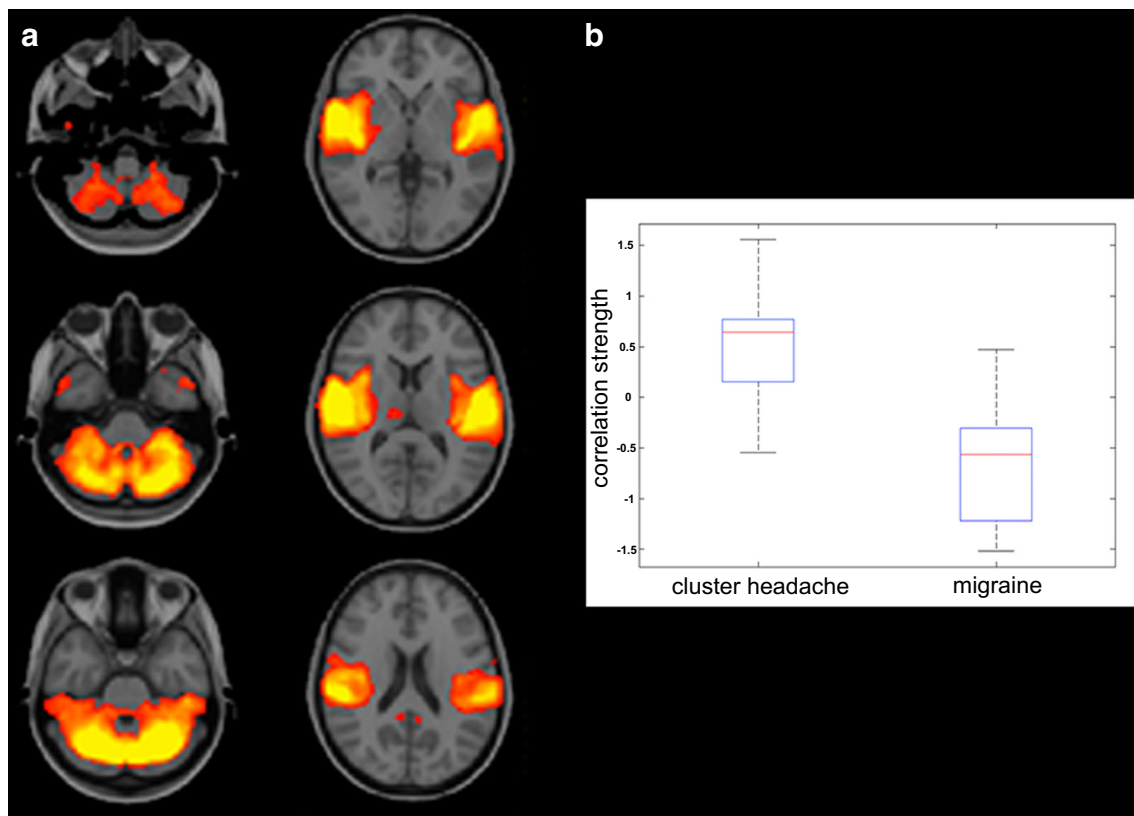


Fig. 3 Differences in internetwork (long-range) functional connectivity between cluster headache and migraine groups. The partial correlation (i.e., direct relationship) between cerebellar network and auditory

language comprehension network (a) was higher (ANOVA, $p \leq 0.01$ corrected) in the former group, as shown by the corresponding box-and-whiskers plots of median and range values (b). See text for details

to Mig patients free from attacks and preventive treatment, and to NC.

CH, compared to NC and Mig, showed decreased regional GM volume in the frontal cortex, a traditional pain processing area, higher short-range functional connectivity in networks subserving working memory and executive functions and, only compared to Mig, higher long-range functional connectivity in language comprehension networks.

Regional GM volume changes

We found decreased regional GM volume in the frontal cortex of CH, mapping on the inferior frontal gyrus compared to NC, in line with a previous study (Yang et al. 2013), and on the frontal pole compared to Mig. This finding has never been shown before, but it fits with the recent hypothesis that, alongside the involvement of posterior hypothalamic and other “classical” nociceptive brain areas, prefrontal areas are involved in the pathophysiology of CH (Sprengr et al. 2007). Decreased GM volume in CH with respect to Mig was also found in a postero-lateral region of the parietal cortex such as the superior lateral occipital cortex which, functionally, represents the site of modulation of visual object processing in the ventral visual stream during pain experience and working memory (Bingel et al. 2007). GM

volume reduction in regions of the prefrontal and postero-parietal cortex of CH with respect to Mig during the interictal phase may overall reflect altered pain-modulating capacity and thus an insufficient structural cortical plasticity towards very severe pain rather than a real process of atrophy due to tissue loss.

Compared only to NC, we also found in CH increased GM volume in the cerebellum, as previously demonstrated (Naegel et al. 2014a), and in a region of the occipital cortex, such as the occipital fusiform gyrus, in agreement with previous studies (Absinta et al. 2012; Naegel et al. 2014b). It is common knowledge that cerebellum is linked with motor sequence generation, sensory-motor control, attention switching and decision making; however, more recent studies suggested a passive role in the response to painful stimuli and, interestingly, also an active role in the cognitive aspects of pain processing. Fusiform gyrus was traditionally linked with various cognitive aspects, including color information processing, face and body recognition, visual object processing, attentional modulation and, more recently, working memory. In pathogenic terms, GM volume increase in the cerebellar and occipital GM of CH with respect to NC may reflect increased regional cortical plasticity and thus a compensatory mechanism aiming to increase or regain pain modulation activity, which may be reduced as a consequence of very severe pain attacks.

Regional GM volume changes, both increase and decrease, as found in our study, were previously reported between in-bout and interictal periods of CH (Naegel et al. 2014b), suggesting that this type of very severe primary headache may actually result from a disordered top-down pain modulatory mechanism, with complex volumetric changes and cortical plasticity dynamics between the different pain states.

Altered functional connectivity

In this study, CH group showed, with respect to both NC and Mig groups, abnormal short- and long-range functional connectivity whereas no group heterogeneity was found for anatomical connectivity along WM tracts.

We showed that higher short-range functional connectivity in CH than in both NC and Mig mapped on regions of the prefrontal cortex, which were part of the working memory network (inferior and middle frontal gyrus, respectively) and executive control network (superior frontal gyrus and frontal pole, respectively).

Interestingly, all alterations in CH with respect to the other two study groups mapped on the right hemisphere, in keeping with the occurrence of right-sided pain in almost all of our CH patients. Our findings on the prefrontal cortex are in line with the occurrence of increased metabolism in the frontal areas of the descending modulation system of the “pain neuromatrix” (Sprenger et al. 2007). Working memory refers to a limited-capacity, short-term, information retention system, necessary for guiding behavior, making decisions, learning a language, reasoning, and planning. Previous studies showed a clinical deficit of working memory in chronic pain patients (Berryman et al. 2013), including those with CH (Torkamani et al. 2015). Besides working memory network, we showed that the executive control network of CH patients had higher functional connectivity than both NC and Mig. The executive control network is a type of attention network that can be selectively influenced by painful stimulation (Liu et al. 2013). However, conflicting results exist on the possible impairment of executive functions in CH patients (Dresler et al. 2012; Torkamani et al. 2015). Finally, when compared only to NC, we found that CH also showed higher functional connectivity in the default mode network. This is a well-known network taking part in internal modes of cognition and activating during internally focused tasks, including memory retrieval. Increased functional connectivity in the default mode network of CH might be directly related to pathophysiology of pain and, indeed, this functional reorganization of the network turned out to be associated with chronic pain conditions (Baliki et al. 2014).

In terms of long-range functional connectivity, we found higher connection strength between the auditory language comprehension network and the cerebellar network in CH compared to Mig, whereas no differences occurred between the two patient groups and NC. The auditory language comprehension network includes the posterior insula, which is part of the ascending processing system of the “pain neuromatrix”,

but also the superior temporal gyrus, whose interaction with the cerebellar network, demonstrated by both task- and resting-FMRI studies (Baumann and Mattingley 2010; Dobromyslin et al. 2012) and confirmed by DTI-derived WM connections (Habas et al. 2011), is involved in an important cognitive task such as language comprehension (McLachlan and Wilson 2017; Moberget and Ivry 2016). In our study, the higher long-range functional connectivity between the cerebellar network and auditory language comprehension network mirror the findings of higher short-range functional connectivity in the working memory network and executive control network of CH compared to Mig and, overall, they may reflect a “maladaptive” (i.e., worsening) process. Indeed, we hypothesize that the very severe pain in CH may initially interfere with the function of brain networks supporting key cognitive abilities, in the absence of clinical cognitive impairment, and this situation may in turn worsen the cognitive and sensory aspects of the pain experience.

There are strengths and limitations to this study. The MRI approaches used for the analyses of GM volumes and connectivity feature important methodological aspects: assessment of the whole brain rather than predefined regions; nonlinear registration, which reduces the potential errors in spatial registration; nonparametric permutation testing, which can be applied when the assumptions of a parametric approach are untenable, as it occurs for small study groups; conservative statistical threshold corrected for multiple comparisons across space, thus protecting against false positive results; and TFCE, which uses the spatial information inherent to the image data for computing statistical maps, thus not requiring arbitrary image presmoothing and not depending on an arbitrary initial cluster-forming threshold.

Limitations lie in the cross-sectional design of the study, which provides only a “snapshot” at a given timepoint, and especially in the small sample size of the study groups, which are, however, in line with most of studies in the field. In addition, we must consider that CH is a rare condition, with a prevalence of around 0.1% in the general population (Hoffmann and May 2018) and that we recruited a selected group of patients not on preventive treatment at the time of the study, well beyond the attack phase and without vascular comorbidities, in order to avoid possible confounders in the interpretation of the results. Future larger prospective studies may contribute to determine whether and how changes in GM volume and functional connectivity are associated with the evolution of CH and Mig. Importantly, our results, which are highly significant in statistical terms, are in favor of the occurrence of real differences in GM volumes and connectivity among the three study groups and, therefore, strongly indicate that additional research should be carried out in the future.

Acknowledgements Riccardo Tappa Brocci (University of Siena) helped with MRI data acquisition; Mary Lokken revised the manuscript for English language editing.

Author's contribution Antonio Giorgio, study concept, acquisition, analysis and interpretation of data, manuscript writing. Chiara Lupi, study concept and design, acquisition of data, manuscript writing. Jian Zhang, acquisition, analysis of data. Francesco De Cesaris, acquisition of data. Mario Alessandri, acquisition of data. Marzia Mortilla, acquisition of data. Antonio Federico, critical revision of manuscript for intellectual content. Pierangelo Geppetti, critical revision of manuscript for intellectual content. Nicola De Stefano, critical revision of manuscript for intellectual content. Silvia Benemei, study concept and design, study supervision, critical revision of manuscript for intellectual content.

Compliance with ethical standards

Conflict of interest The authors declare no conflict of interest specific for this study.

Ethical approval All procedures performed in this study were in accordance with the ethical standards of the local Institutional Ethics Committee on Clinical Research and with the Helsinki Declaration (version amended during the 64th WMA General Assembly, Fortaleza, Brazil, October 2013). Written informed consent was obtained from all participants before study entry.

Publisher's note Springer Nature remains neutral with regard to jurisdictional claims in published maps and institutional affiliations.

References

- (IHS) HCCotIHS. (2013). The international classification of headache disorders, 3rd edition (beta version). *Cephalalgia*, 33(9), 629–808.
- Absinta, M., Rocca, M. A., Colombo, B., Falini, A., Comi, G., & Filippi, M. (2012). Selective decreased grey matter volume of the pain-matrix network in cluster headache. *Cephalalgia*, 32(2), 109–115.
- Arkink, E. B., Schmitz, N., Schoonman, G. G., van Vliet, J. A., Haan, J., van Buchem, M. A., Ferrari, M. D., & Kruit, M. C. (2017). The anterior hypothalamus in cluster headache. *Cephalalgia*, 37(11), 1039–1050.
- Baliki, M. N., Mansour, A. R., Baria, A. T., & Apkarian, A. V. (2014). Functional reorganization of the default mode network across chronic pain conditions. *PLoS One*, 9(9), e106133.
- Baumann, O., & Mattingley, J. B. (2010). Scaling of neural responses to visual and auditory motion in the human cerebellum. *The Journal of Neuroscience*, 30(12), 4489–4495.
- Berryman, C., Stanton, T. R., Jane Bowering, K., Tabor, A., McFarlane, A., & Lorimer Moseley, G. (2013). Evidence for working memory deficits in chronic pain: a systematic review and meta-analysis. *Pain*, 154(8), 1181–1196.
- Bingel, U., Rose, M., Glascher, J., & Buchel, C. (2007). fMRI reveals how pain modulates visual object processing in the ventral visual stream. *Neuron*, 55(1), 157–167.
- Chen, Z., Chen, X., Liu, M., Liu, S., Shu, S., Ma, L., & Yu, S. (2016). Altered functional connectivity of the marginal division in migraine: a resting-state fMRI study. *The Journal of Headache and Pain*, 17(1), 89.
- Chou, K. H., Yang, F. C., Fuh, J. L., Huang, C. C., Lim, J. F., Lin, Y. Y., Lee, P. L., Kao, H. W., Lin, C. P., & Wang, S. J. (2014). Altered white matter microstructural connectivity in cluster headaches: a longitudinal diffusion tensor imaging study. *Cephalalgia*, 34(13), 1040–1052.
- Dobromylin, V. I., Salat, D. H., Fortier, C. B., Leritz, E. C., Beckmann, C. F., Milberg, W. P., & McGlinchey, R. E. (2012). Distinct functional networks within the cerebellum and their relation to cortical systems assessed with independent component analysis. *Neuroimage*, 60(4), 2073–2085.
- Dresler, T., Lurding, R., Paelecke-Habermann, Y., Gaul, C., Henkel, K., Lindwurm-Spath, A., Leinisch, E., & Jurgens, T. P. (2012). Cluster headache and neuropsychological functioning. *Cephalalgia*, 32(11), 813–821.
- Fazekas, F., Chawluk, J. B., Alavi, A., Hurtig, H. I., & Zimmerman, R. A. (1987). MR signal abnormalities at 1.5 T in Alzheimer's dementia and normal aging. *AJR. American Journal of Roentgenology*, 149(2), 351–356.
- Granziera, C., DaSilva, A. F., Snyder, J., Tuch, D. S., & Hadjikhani, N. (2006). Anatomical alterations of the visual motion processing network in migraine with and without aura. *PLoS Medicine*, 3(10), e402.
- Habas, C., Guillemin, R., & Abanou, A. (2011). Functional connectivity of the superior human temporal sulcus in the brain resting state at 3T. *Neuroradiology*, 53(2), 129–140.
- Hadjipavlou, G., Duncley, P., Behrens, T. E., & Tracey, I. (2006). Determining anatomical connectivities between cortical and brainstem pain processing regions in humans: a diffusion tensor imaging study in healthy controls. *Pain*, 123(1–2), 169–178.
- Hoffmann, J., & May, A. (2018). Diagnosis, pathophysiology, and management of cluster headache. *Lancet Neurology*, 17(1), 75–83.
- Jenkinson, M., & Smith, S. (2001). A global optimisation method for robust affine registration of brain images. *Medical Image Analysis*, 5(2), 143–156.
- Jin, C., Yuan, K., Zhao, L., Yu, D., von Deneen, K. M., Zhang, M., Qin, W., Sun, W., & Tian, J. (2013). Structural and functional abnormalities in migraine patients without aura. *NMR in Biomedicine*, 26(1), 58–64.
- Kim, J. H., Suh, S. I., Seol, H. Y., Oh, K., Seo, W. K., Yu, S. W., Park, K. W., & Koh, S. B. (2008). Regional grey matter changes in patients with migraine: a voxel-based morphometry study. *Cephalalgia*, 28(6), 598–604.
- Liu, G., Ma, H. J., Hu, P. P., Tian, Y. H., Hu, S., Fan, J., & Wang, K. (2013). Effects of painful stimulation and acupuncture on attention networks in healthy subjects. *Behavioral and Brain Functions*, 9, 23.
- McLachlan, N. M., & Wilson, S. J. (2017). The contribution of brainstem and cerebellar pathways to auditory recognition. *Frontiers in Psychology*, 8, 265.
- Messina, R., Rocca, M. A., Colombo, B., Valsasina, P., Horsfield, M. A., Copetti, M., Falini, A., Comi, G., & Filippi, M. (2013). Cortical abnormalities in patients with migraine: a surface-based analysis. *Radiology*, 268(1), 170–180.
- Moberget, T., & Ivry, R. B. (2016). Cerebellar contributions to motor control and language comprehension: searching for common computational principles. *Annals of the New York Academy of Sciences*, 1369(1), 154–171.
- Naegel, S., Holle, D., Desmarattes, N., Theysohn, N., Diener, H. C., Katsarava, Z., & Obermann, M. (2014a). Cortical plasticity in episodic and chronic cluster headache. *NeuroImage: Clinical*, 6, 415–423.
- Naegel, S., Holle, D., & Obermann, M. (2014b). Structural imaging in cluster headache. *Current Pain and Headache Reports*, 18(5), 415.
- Neeb, L., Bastian, K., Villringer, K., Gits, H. C., Israel, H., Reuter, U., & Fiebich, J. B. (2015). No microstructural white matter alterations in chronic and episodic migraineurs: a case-control diffusion tensor magnetic resonance imaging study. *Headache*, 55(2), 241–251.
- Oguz, I., Farzinfar, M., Matsui, J., Budin, F., Liu, Z., Gerig, G., Johnson, H. J., & Styner, M. (2014). DTIPrep: quality control of diffusion-weighted images. *Frontiers in Neuroinformatics*, 8, 4.
- Pruim, R. H., Mennes, M., van Rooij, D., Llera, A., Buitelaar, J. K., & Beckmann, C. F. (2015). ICA-AROMA: a robust ICA-based strategy for removing motion artifacts from fMRI data. *Neuroimage*, 112, 267–277.
- Qiu, E., Wang, Y., Ma, L., Tian, L., Liu, R., Dong, Z., Xu, X., Zou, Z., & Yu, S. (2013). Abnormal brain functional connectivity of the hypothalamus in cluster headaches. *PLoS One*, 8(2), e57896.

- Rocca, M. A., Ceccarelli, A., Falini, A., Colombo, B., Tortorella, P., Bernasconi, L., Comi, G., Scotti, G., & Filippi, M. (2006). Brain gray matter changes in migraine patients with T2-visible lesions: a 3-T MRI study. *Stroke*, *37*(7), 1765–1770.
- Sprenger, T., Ruether, K. V., Boecker, H., Valet, M., Berthele, A., Pfaffenrath, V., Woller, A., & Tolle, T. R. (2007). Altered metabolism in frontal brain circuits in cluster headache. *Cephalalgia*, *27*(9), 1033–1042.
- Szabo, N., Kincses, Z. T., Pardutz, A., Toth, E., Szok, D., Csete, G., & Vecsei, L. (2013). White matter disintegration in cluster headache. *The Journal of Headache and Pain*, *14*, 64.
- Teepker, M., Menzler, K., Belke, M., Heverhagen, J. T., Voelker, M., Mylius, V., Oertel, W. H., Rosenow, F., & Knake, S. (2012). Diffusion tensor imaging in episodic cluster headache. *Headache*, *52*(2), 274–282.
- Torkamani, M., Ernst, L., Cheung, L. S., Lambrou, G., Matharu, M., & Jahanshahi, M. (2015). The neuropsychology of cluster headache: cognition, mood, disability, and quality of life of patients with chronic and episodic cluster headache. *Headache*, *55*(2), 287–300.
- Valfre, W., Rainero, I., Bergui, M., & Pinessi, L. (2008). Voxel-based morphometry reveals gray matter abnormalities in migraine. *Headache*, *48*(1), 109–117.
- Yang, F. C., Chou, K. H., Fuh, J. L., Huang, C. C., Limg, J. F., Lin, Y. Y., Lin, C. P., & Wang, S. J. (2013). Altered gray matter volume in the frontal pain modulation network in patients with cluster headache. *Pain*, *154*(6), 801–807.
- Yang, F. C., Chou, K. H., Fuh, J. L., Lee, P. L., Limg, J. F., Lin, Y. Y., Lin, C. P., & Wang, S. J. (2014). Altered hypothalamic functional connectivity in cluster headache: a longitudinal resting-state functional MRI study. *Journal of Neurology, Neurosurgery, and Psychiatry*, *86*(4), 437–445.
- Yu, D., Yuan, K., Qin, W., Zhao, L., Dong, M., Liu, P., Yang, X., Liu, J., Sun, J., Zhou, G., von Deneen, K. M., & Tian, J. (2013). Axonal loss of white matter in migraine without aura: a tract-based spatial statistics study. *Cephalalgia*, *33*(1), 34–42.
- Yu, Z. B., Lv, Y. B., Song, L. H., Liu, D. H., Huang, X. L., Hu, X. Y., Zuo, Z. W., Wang, Y., Yang, Q., Peng, J., Zhou, Z. H., & Li, H. T. (2017). Functional connectivity differences in the insular sub-regions in migraine without Aura: a resting-state functional magnetic resonance imaging study. *Frontiers in Behavioral Neuroscience*, *11*, 124.
- Yuan, K., Qin, W., Liu, P., Zhao, L., Yu, D., Dong, M., Liu, J., Yang, X., von Deneen, K. M., Liang, F., & Tian, J. (2012). Reduced fractional anisotropy of corpus callosum modulates inter-hemispheric resting state functional connectivity in migraine patients without aura. *PLoS One*, *7*(9), e45476.